The mutual influence of Y···N and H···H interactions in XHY···NCH···HM complexes (X=F, Cl, Br; Y=S, Se; M=Li, Na, BeH, MgH): Tuning of the chalcogen bond by dihydrogen bond interaction

Mehdi D. Esrafili[*,a], Soheila Asadollahi [a] and Yousef Dadban Shahamat [b]

[a] *Laboratory of Theoretical Chemistry, Department of Chemistry, University of Maragheh, Maragheh, Iran*

[b] *Environmental Heath Research Center, Golestan University of Medical Sciences, Gorgan, Iran*

* Corresponding Author. **Phone:** (+98) 4212237955. **Fax:** (+98) 4212276060. **P.O. Box:** 5513864596. **E-mail**: esrafili@maragheh.ac.ir.

Abstract

The equilibrium structures, interaction energies and bonding properties of ternary XHY···NCH···HM complexes are studied by ab initio calculations, where X=F, Cl, Br; Y=S, Se and M=Li, Na, BeH and MgH. The ab initio calculations are carried out at the MP2/aug-cc-pVTZ level. The results indicate that all optimized Y···N and H···H binding distances in the ternary complexes are smaller than the corresponding values in the binary systems. The calculated cooperative energies (E_{coop}) are between -0.20 kcal/mol in the BrHS···NCH···HBeH and -3.29 kcal/mol in the FHSe···NCH···HNa. For given Y and M, the estimated E_{coop} values increase as X= F > Cl > Br. In addition, the Se-bonded complexes exibit a larger E_{coop} values than those of S-bonded counterparts. The cooerativity between Y···N and H···H interactions is further analyzed by quantum theory of atoms in molecules and natural bond orbital methods. Cooperative effects make an increase in the J(Y–N) and J(H–H) spin-spin coupling constants of the ternary complexes with respect to the binary systems.

Key words: chalcogen bond; electrostatic potential; ab initio; cooperativity; NMR.

1. Introduction

Noncovalent interactions play an important role in various fields of chemistry and biochemistry. The biological activities of most macromolecules like proteins and polypeptides in living cells are largely controlled by the noncovalent interactions [1-2]. Of the various noncovalent bonds, the hydrogen bond (HB) is undoubtedly the most thoroughly studied case. The classical HB is generally formulated as an attractive A−H···B interaction, in which the H atom acts as a bridge between the two electronegative atoms (A, B= F, O and N). There are also so-called nonclassical HBs, like C−H···N, S−H···N or even C−H···C [3]. Dihydrogen bond (DHB) [4-8] is a special type of nonclassical HBs in which the negative charged H atom acts as a proton acceptor. This interaction is commonly characterized by an unusually short H···H binding distance that is less than or equal to the sums of the van der Waals (vdW) radii of the two hydrogen atoms (1.2 Å) [9], and a normally linear A−H···H arrangement. Besides HBs, there are also other important noncovalent interactions. Halogen bonding [10-12] is a noncovalent interaction similar to the HB, in which a halogen atom serves a similar function as a bridge between two molecules. This is very surprising since covalently-bonded halogen atoms are generally viewed as being negatively charged and thus would not be expected to interact attractively with other negative site. Nevertheless, a detailed analysis of the electrostatic potential around the halogen atoms revealed the existence of an electron-deficient region, called as "σ-hole" by Politzer and coworkers [13-22], which is directed toward the negative site on the electron donor. The presence or absence of the σ-hole and its magnitude depend upon several factors, including the polarizability and electronegativity of the halogen atom and the electron-withdrawing ability of the remainder of the molecule. For a given negative site, the strength of halogen bonds usually correlates with the magnitudes of the σ-hole potential on the halogen, that is, the more polarizable halogen atoms (Br and I) tends to form stronger halogen bonds than less polarizable ones (F and Cl).

Work over the years has indicated that the σ-hole concept can be also extended to the covalently-bonded Group 14-16 atoms [21, 23-24]. For instance, there are extensive theoretical [25-30] and experimental [31-32] studies that indicate the Group 16 atoms (chalcogen group) are able to form σ-hole bond interaction with potential negative sites. The resulting "chalcogen bond" is highly directional and is comparable in strength to that of the HB or halogen bond [33-36]. The tendency to form chalcogen bonds with Lewis bases increases in the order of S < Se < Te. Like

halogen bonds, chalcogen bonds share fundamental characteristics with the HB. For example, although the stability of the chalcogen bonding is mainly due to the electrostatic effects [29, 34, 37], but mutual polarization of chalcogen bond donor and acceptor, charge-transfer [33-34, 38-39] and dispersion energies [40-41] have also significant contributions. Moreover, the strength of chalcogen bonds can be tuned by substitution effects, i.e. an electron-withdrawing group in the chalcogen donor tends to increase the strength of the chalcogen bond. And finally, they show cooperative effects with itself [42] and other types of interactions [42-43].

When two or more noncovalent interactions coexist in a multicomponent system, they will mutually influence each other and therefore a cooperative effect may be occurred between them [44]. Such a situation is relevant in biomacromolecules like proteins, where various types of noncovalent interactions may coexist [45]. The cooperative effect between these noncovalent interactions is expected to responsible for some interesting energetic and geometric effects in these systems. Thus, a detailed understanding of these cooperative effects is of great importance for the interpretation of many physical and chemical properties of biomocromolecules in biological systems. For example, the interplay between chalcogen bond and halogen bond interactions was recently reported. Zhao [46] showed that for a series of model of chalcogen- and halogen-bonded complexes $XCl\cdots OCS\cdots NH_3$ (X= F, OH, NC, CN, and FCC), cooperative effects tend to strengthen the interactions. A recent theoretical study by our group [47] also indicated that the ordering of the monomers in ternary complexes M^+–PhYH–NH_3, M^+–PhYH–NCH and M^+–PhCCCN–YHF (Ph=phenyl; M=Li, Na; Y=Se, Te) has an important effects on the cooperativity between the chalcogen bond and cation-π interactions.

In the present study, we investigate the geometries, interaction energies and bonding properties of some ternary complexes connected by chalcogen and DHB interactions. We selected XHY···NCH···HM complexes, where X=F, Cl, Br; Y=S, Se and M=Li, Na, BeH and MgH. In order to characterize the nature of the interactions, molecular electrostatic (MEP), quantum theory of atoms in molecules (QTAIM) and natural bond orbital (NBO) were performed. We believe that the results of the present study can be useful for the extension and future applications of the chalcogen bonds as a useful tool for design and synthesis of supramolecular systems with desired properties.

2. Computational details

The geometry optimizations and the corresponding harmonic frequency calculations were carried out at the MP2/aug-cc-pVTZ level of theory using GAMESS [48] electronic structure package. No imaginary frequency was found for any of the structures determined, so they are true minima. The interaction energy was calculated at the MP2/aug-cc-pVTZ level as the difference of the total energy of the complexes and the sum of the isolated monomers in their complex geometry. The basis set superposition error (BSSE) calculated with the counterpoise (CP) method [49] was used to correct the interaction energies.

The molecular electrostatic potentials (MEPs) were computed on the 0.001 electrons/Bohr^3 contour of the electronic density using the Wave Function Analysis-Surface Analysis Suite (WFA-SAS) [50]. NBO analysis [51] was performed by the NBO 5.0 program [52]. Since MP2 orbitals are nonexistent, the charge transfer energies were evaluated at HF/aug-cc-pVTZ level. The QTAIM [53] analysis was performed with the help of AIM2000 program [54] by using the wave functions generated at the MP2/aug-cc-pVTZ level of theory. The ^{1}H and ^{15}N chemical shielding isotropy values as well as spin-spin coupling constant across the chalcogen bond and DHB interactions were calculated with the gauge-included atomic orbital (GIAO) approach.

3. Results and discussion

3.1. Isolated monomers

We first focus on the MEP map of the isolated monomers, since prior studies [56-58] have demonstrated the importance of this analysis as a powerful tool for predicting the active Lewis acid/base sites around a molecule. The calculated electrostatic potential maximum ($V_{S,max}$) and minimum ($V_{S,min}$) values of the isolated molecules are listed in Table 1. Figure 1 indicates the MEP maps, on the 0.001 electrons/bohr^3 contour, of the SHF, NCH, LiH and HBeH molecules. As it is evident, the MEP of SHF shows an area of positive potential (σ-hole), located at the outer side of the S atom, along the S−F bond. This σ-hole is formed because the electron density around the S atom is drawn sufficiently toward the more negative F atom and hence a region of depletion of electronic density is created on the side of the S opposite to the S–F bond. From Table 1, one can see that for a given X substitution, the $V_{S,max}$ value associated with the Se atom of SeHX is larger than that of SHX counterpart, which is due to the smaller electronegativity and larger polarizability of the Se atom than S. In the case of NCH, there is a distinct positive MEP

region on the hydrogen atom which indicates its propensity for the formation of a HB interaction. The latter positive area is characterized by a $V_{S,max}$ value of 58.7 kcal/mol. Besides, the MEP of this molecule exhibits a negative region on the nitrogen atom, corresponding to the lone-pair of electrons on this atom. Consequently, the NCH molecule can simultaneously play a dual role of Lewis acid and base. Considering the MEP map of the LiH and HBeH molecules (Figure 1), it is seen that there is a negative MEP region ($V_{S,min}$) on the outermost portion of the H surface along the Li–H or Be–H bond. The calculated $V_{S,min}$ values are -53.0, -56.9, -13.6 and -24.8 kcal/mol for the LiH, NaH, HBeH and HMgH molecules, respectively. Thus, the hydrogen atom in these molecules can act as a potential negative site for an electrophilic attack, which has been previously evidenced in numerous σ-hole bonded complexes [59-61].

3.2. Binary and ternary complexes

Geometries. Table 2 summarizes the Y···N and H···H binding distances in the binary XHY···NCH and NCH···HM complexes. The corresponding optimized structures are given in Figure S1 of the Supporting Information. The estimated Y···N distances in the XHY···NCH complexes are between 2.566 and 2.888 Å. It is seen that for a given Y atom, the chalcogen bond distances in the XHY···NCH increase as the size of the halogen atom increases. The chalcogen atom type has also a significant effect on the Y···N binding distances and for a given X substitution, the SeHX molecules tend to form shorter chalcogen bonds than SHX counterparts. This finding is consistent with the estimated $V_{S,max}$ values obtained on these atoms (Table 1). All of the chalcogen bonds have a favorable linear arrangement, with $\angle$X−Y···N values between 165 and 170°. On the other hand, the calculated H···H distances are 1.773, 1.760, 2.030 and 1.924 Å in the NCH···HLi, NCH···HNa, NCH···HBeH and NCH···HMgH binary complexes, respectively. All these binding distances are much smaller than the sum of the vdW radii of two hydrogen atoms (about 2.40 Å) [9], which verifies the formation of an attractive DHB interaction in these complexes. From Figure S1, it is also seen that all optimized equilibrium C–H···H interactions in the NCH···HM complexes are essentially linear, which can be explained by the MEPs of the isolated HCN and HM molecules as noted above.

The optimized structures of the ternary XHY···NCH···HM complexes are shown in Figure S2 of Supporting Information. The Y···N and H···H binding distances and their variation (ΔR) with respect to the binary complexes are listed in Table 2. It is evident that the Y···N and

H···H distances in the ternary complexes are always shorter than the corresponding values in the binary systems. This means that there exists a cooperativity between these interactions in the ternary complexes. One can also see that for the M=Li and Na complexes, the shortening of the Y···N binding distances is more important than that in the H···H, while a reverse trend is obtained for the M=BeH and MgH systems. The differences in distances between ternary and binary complexes are in the range of 0.020–0.136 Å and 0.033–0.123 Å for the Y···N and H···H interactions, respectively (Table 2). In addition, the effect of the H···H interaction on the S···N interaction is more prominent than on the Se···N one. This is consistent with a series of earlier reports [43, 58, 62] which show that in a ternary complex, the strong interaction has a great influence on the weak one.

Interaction energies. The BSSE-corrected interaction energies of the binary and ternary complexes are listed in Table 3. These are calculated as the difference of the total energy of the complexes and the sum of the isolated monomers in their complex geometry. The estimated interaction energies of the binary XHY···NCH complexes are in the range -3.45 to -6.69 kcal/mol, which are in good agreement with those of other reported chalcogen-bonded complexes in literature [33-34, 36, 63]. For a given Y, the interaction energy becomes more negative in the order X= F > Cl > Br. This is the order of increasing positive electrostatic potential on the Y atom, which supports the conclusion that the electrostatic effects play an important role in the formation of the Y···N interactions. The interaction energies of NCH···HM complexes range from -2.01 to -9.68 kcal/mol and becomes more negative in the order M= Na > Li > MgH > BeH. This finding is almost consistent with the magnitude of the $V_{S,min}$ values associated with the H atom of HM (Table 1), and clearly indicates the electrostatic nature of these DHB interactions.

Table 3 also gives the Y···N and H···H interaction energies in the ternary systems. These are calculated as the total energy of a triad minus the energy sum of the corresponding isolated binary complexes. For example, E_{int} (AB, T)=E_{ABC} − (E_A + E_{BC}) − E_{int} (AC, T), where E_{ABC} means the total energy of the triad, E_A is the energy of the isolated A monomer, E_{BC} is the energy of the BC dyad and E_{int} (AC, T) is the interaction energy of the AC pair in the geometry of triad. All these energies are corrected for BSSE. From Table 3 results, it is evident that the addition of HM molecule to the XHY···NCH always increases the strength of the Y···N bond, but the nature of the substitution X determines the extent of the increase. That is, the weaker chalcogen bond

suffers a much bigger enhancement than the stronger one. Our results also indicate that the formation of the Y···N bond has an important influence on the weak DHB interactions. These results are consistent with the shortening of the binding distances as discussed above and support the view that in a ternary complex, the strong interaction has a great cooperative effect on the weak one.

Table 3 also shows the cooperative energies (E_{coop}) in the ternary complexes as the consequence of the coexistence of both Y···N and H···H interactions. It is obtained as:

$$E_{coop} = E_{int}(ABC) - E_{int}(AB) - E_{int}(BC) - E_{int}(AC, T) \quad (1)$$

where $E_{int}(ABC)$ is the interaction energy of the trimer, $E_{int}(AB)$ and $E_{int}(BC)$ are the interaction energies of the isolated dimers within their corresponding minima configurations. The last term, E_{int} (AC, T), indicates the interaction energy of AC pairs, within the geometry of the trimer. From Table 3, it is seen that the E_{coop} values are all negative, which means that the interaction energy of the ternary complex is greater (more negative) than the sum of the interaction energies of the corresponding binary complexes. The calculated E_{coop} values are between -0.20 kcal/mol in the BrHS···NCH···HBeH and -3.29 kcal/mol in the FHSe···NCH···HNa. It is interesting to note that for given Y and M, the estimated E_{coop} values decreases as X= F > Cl > Br. The Se-bonded complexes show also a larger E_{coop} values than those of S-bonded counterparts. From Table 3 results, one can see that the E_{coop} values are modest for the HBeH and HMgH complexes due to their weak H···H interactions. Yet, cooperative effects between the two interactions contribute 4–9% of the total interaction energies of these complexes.

Electron density analysis. The topology analysis of the electron density by means of the QTAIM method provides useful tools to confirm the formation of the Y···N and H···H interactions in the title complexes. Table 4 summarizes the calculated electron density (ρ_{BCP}) and the corresponding Laplacian ($\nabla^2\rho_{BCP}$) values computed at the Y···N and H···H bond critical points (BCPs) of the complexes. It has been shown in numerous studies [64-66] that the ρ_{BCP} gives valuable information about the strength and origin of the interactions. Hence, the variation in the ρ_{BCP} value at the BCPs in the triads with respect to the corresponding dyads can be used to analyze the mutual influence of the two interactions. The values of ρ_{BCP} at the Y···N critical points of the XHY···NCH···HM complexes are in the range of 0.014–0.035 au, which fall in the generally accepted range of a HB (0.002–0.035) au [67]. In addition, their corresponding $\nabla^2\rho_{BCP}$

values (0.060–0.116 au) fall in the proposed range of a HB [67]. These findings indicate that the all S···N and Se···N chalcogen bonds studied here are weak and mainly electrostatic in nature. For the H···H interactions, both ρ_{BCP} and $\nabla^2\rho_{BCP}$ values follow the same order with the interaction energies. It is also seen that the capacity of the XHY···NCH···HM complexes to concentrate electrons at the Y···N and H···H BCPs increases significantly with the size of Y atom. As a matter of fact, an exponential relationship is found between the binding distances and electron densities at BCPs of the ternary complexes (Figure 2), which is similar to other related studies [29, 37]. On the other hand, the results of Table 4 show that the ρ_{BCP} and $\nabla^2\rho_{BCP}$ values at the Y···N and H···H critical points in the triads are slightly larger than that in the corresponding dyads. This finding is quite expected and confirms that the both interactions in the ternary systems are reinforced with respect to the binary ones.

NBO analysis. Another valuable method to analyze the cooperativity of the chalcogen bond and DHB interactions in the ternary complexes is the NBO theory. Table 5 gives the calculated NBO stabilization energies ($E^{(2)}$) and net charge-transfer (Q_{CT}) values associated with the formation of Y···N and H···H interactions in the binary and ternary complexes. The formation of each Y···N interaction is associated by an electron charge transfer from the lone pair of the nitrogen atom to the σ^*_{Y-X} antibonding orbital of YHX molecule. In the case of NCH···HM complexes, the main interaction responsible for the stabilization of these systems arises from the second-order orbital interaction of the bonding σ_{M-H} orbital of the HM with the σ^*_{C-H} acceptor orbital of NCH. One can see that for the XHY···NCH and NCH···HM binary complexes, the $E^{(2)}$ values follow the same order with the interaction energies. Also, the $E^{(2)}$ values in the Y···N and H···H interactions of the XHY···NCH···HM complexes are always larger than those of binary systems. This confirms that both interactions are reinforced in the ternary complexes. For instance, the estimated $E^{(2)}$ values in the Y···N interaction of XHY···NCH···HM complexes are in the range of 3.91-25.18 kcal/mol, which are 0.33-8.71 kcal/mol larger than those of binary XHY···NCH complexes. As evident, the largest increase in the $E^{(2)}$ value associated with the Y···N and H···H bonds occurs for the complex FHSe···NCH···HNa, which exhibits the largest E_{coop} value as noted above.

It is also expected that the strong cooperativity between the Y···N and H···H interactions is reflected in the magnitude of the charge transfer values (Q_{CT}). These Q_{CT} are given in Table 5,

and are obtained according to the predicted NBO atomic charges of the interacting molecules. The examination of Table 5 results reveals that there is a clear relationship between the interaction energies and Q_{CT} values, i.e. the stronger the Y···N or H···H interaction, the larger corresponding Q_{CT} value. Hence, the variation in the Q_{CT} values in the ternary systems with respect to the corresponding dyads can be used to analyze the mutual influence of the two interactions. It is evident from Table 5 that the Q_{CT} value associated with the Y···N and H···H interactions of the triads are slightly greater than those of the corresponding dyads. This finding provides another proof for the enhancement of the strength of these interactions in the ternary complexes with respect to the binary ones. As expected, the SeHX complexes exhibit a larger increase in the Q_{CT} values than the SHX ones. In particular, the Q_{CT} value associated with the chalcogen bond of the FHSe···NCH···NCH···HNa complex increases by 52% compared to the FHSe···NCH system.

NMR properties. Table 6 lists the absolute ^{15}N and ^{1}H isotropic chemical shielding (σ) values of NCH molecule in the binary and ternary complexes. The calculated $\sigma(^{15}N)$ values in the binary XHY···NCH complexes are between 61.4 and 74.3 ppm, and show a clear dependency on the Y···N interaction energies. The estimated $\sigma(^{1}H)$ value of NCH molecule in the binary NCH···HM complexes range from 23.8 to 28.5 ppm and tend to decrease as the strength of the DHB interaction increases. The results of Table 6 also indicate that both $\sigma(^{15}N)$ and $\sigma(^{1}H)$ values in the ternary systems are always smaller than those in the respective dyads. This trend can be also interpreted as a cooperative effect between the Y···N and H···H interactions. As expected, these effects are larger in those complexes with stronger cooperative interactions than in those with the weaker ones.

Table 6 also lists the total spin-spin coupling constants across the chalcogen bond, J(Y–N), and DHB interaction, J(H–H), of the binary and ternary complexes. As evident, both J(Y–N) and J(H–H) values in the binary complexes span almost a narrow range. For example, the estimated J(Y–N) value in the dimer BrHS···NCH is 8.7 Hz, and increases by 4 Hz in the FHS···NCH. The type of the Y atom has also an influence on the J(Y–N) values. That is, the calculated J(Y–N) values tend to increase as the size of the Y atom increases. The results of Table 6 shows that the cooperative effects in electronic structure induced by the formation of the Y···N and H···H bonds can influence the J(Y–N) and J(H–H) values in the ternary complexes. In

all the ternary systems, cooperative effects make an increase in the J(Y–N) and J(H–H) coupling constants. This is another evidence for the strengthening of the Y···N and H···N interactions in the ternary complexes with respect to the binary systems. For given Y and M, the values of J(Y–N) and J(H–H) decrease in the order X=F > Cl > Br, which is in line with the calculated total interaction energies of these complexes.

4. Conclusion

An ab initio study was performed at the MP2/aug-cc-pVTZ level of theory to investigate the mutual influence between the chalcogen bond and DHB interactions in the ternary XHY···NCH···HM complexes, where X=F, Cl, Br; Y=S, Se; M=Li, Na, BeH and MgH. The examination of binding distances and interaction energies suggested that both the Y···N and H···H interactions are reinforced by the cooperative effects in the ternary complexes. The differences in distances between ternary and binary complexes are in the range of 0.020–0.136 Å and 0.033–0.123 Å for the Y···N and H···H interactions, respectively. It is found that the addition of the HM molecule to the XHY···NCH always increases the strength of the Y···N bond. In addition, the weaker chalcogen bond suffers a much bigger enhancement than the stronger one. The ρ_{BCP} and $\nabla^2\rho_{BCP}$ values at the Y···N and H···H BCPs in the triads are slightly greater than that in the corresponding dyads. Also, the charge-transfer stabilization energies, $E^{(2)}$, in the Y···N and H···H interactions of the XHY···NCH···HM complexes were found to be larger than those of the binary systems. These results indicated that the strength of these interactions in the ternary complexes is reinforced with respect to the binary ones. Cooperative effects were found to decrease the ^{15}N and ^{1}H isotropic chemical shielding values of the NCH molecule in the ternary complexes. The amount of the cooperativity effects on the J(Y–N) and J(H–H) values depends on the strength of the Y···N and H···H interactions. The results of this study may be helpful for the extension of the chalcogen bonds as a valuable tool for design and synthesis of supramolecular assemblies with desired properties.

References

1. Müller-Dethlefs, K.; Hobza, P., *Chem. Rev.* **2000,** *100* (1), 143.
2. Nick, T. U.; Lee, W.; Koßmann, S.; Neese, F.; Stubbe, J.; Bennati, M., *J. Am. Chem. Soc.* **2015,** *137* (1), 289.
3. Scheiner, S. *Hydrogen bonding. A theoretical perspective*. Oxford University Press: New York, 1997.
4. Bonds, U. H., *J. Am. Chem. Soc.* **1995,** *117* (51), 12875.
5. McDowell, S. A. C.; Forde, T. S., *J. Chem. Phys.* **2002,** *117* (13), 6032.
6. McDowell, S. A. C., *J. Chem. Phys.* **2004,** *121* (12), 5728.
7. Alkorta, I.; Zborowski, K.; Elguero, J.; Solimannejad, M., *J. Phys. Chem. A* **2006,** *110* (34), 10279.
8. Solimannejad, M.; Alkorta, I., *Chem. Phys.* **2006,** *324* (2), 459.
9. Bondi, A., *J. Phys. Chem.* **1964,** *68* (3), 441.
10. Pavan, M. S.; Prasad, K. D.; Row, T. G., *Chem. Commun.* **2013,** *49* (68), 7558.
11. Troff, R. W.; Mäkelä, T.; Topić, F.; Valkonen, A.; Raatikainen, K.; Rissanen, K., *Eur. J. Org. Chem.* **2013,** *2013* (9), 1617.
12. Esrafili, M. D.; Solimannejad, M., *Can. J. Chem.* **2014,** *92* (1), 33.
13. Clark, T.; Hennemann, M.; Murray, J. S.; Politzer, P., *J. Mol. Model.* **2007,** *13* (2), 291.
14. Politzer, P.; Murray, J. S.; Lane, P., *Int. J. Quantum Chem.* **2007,** *107* (15), 3046.
15. Murray, J. S.; Concha, M. C.; Lane, P.; Hobza, P.; Politzer, P., *J. Mol. Model.* **2008,** *14* (8), 699.
16. Politzer, P.; Murray, J. S.; Concha, M. C., *J. Mol. Model.* **2008,** *14* (8), 659.
17. Murray, J. S.; Riley, K. E.; Politzer, P.; Clark, T., *Aust. J. Chem.* **2010,** *63* (12), 1598.
18. Politzer, P.; Murray, J. S.; Clark, T., *Phys. Chem. Chem. Phys.* **2010,** *12* (28), 7748.
19. Murray, J. S.; Politzer, P., *Wiley Interdisciplinary Reviews: Computational Molecular Science* **2011,** *1* (2), 153.
20. Murray, J. S.; Lane, P.; Clark, T.; Riley, K. E.; Politzer, P., *J. Mol. Model.* **2012,** *18* (2), 541.
21. Politzer, P.; Murray, J. S.; Clark, T., *Phys. Chem. Chem. Phys.* **2013,** *15* (27), 11178.
22. Murray, J. S.; Macaveiu, L.; Politzer, P., *J. Comput. Sci.* **2014,** *5* (4), 590.
23. Murray, J. S.; Lane, P.; Politzer, P., *J. Mol. Model.* **2009,** *15* (6), 723.
24. Bundhun, A.; Ramasami, P.; Murray, J.; Politzer, P., *J. Mol. Model.* **2013,** *19* (7), 2739.
25. Wang, W.; Ji, B.; Zhang, Y., *J. Phys. Chem. A* **2009,** *113* (28), 8132.
26. Li, Q.-Z.; Li, R.; Guo, P.; Li, H.; Li, W.-Z.; Cheng, J.-B., *Comput. Theor. Chem.* **2012,** *980*, 56.

27. Adhikari, U.; Scheiner, S., *J. Phys. Chem. A* **2014,** *118* (17), 3183.
28. Azofra, L. M.; Scheiner, S., *J. Phys. Chem. A* **2014,** *118* (21), 3835.
29. Esrafili, M. D.; Mohammadian-Sabet, F., *Chem. Phys. Lett.* **2015,** *634*, 210.
30. Esrafili, M. D.; Mohammadian-Sabet, F., *J. Mol. Model.* **2015,** *21* (3), 65.
31. Brezgunova, M. E.; Lieffrig, J.; Aubert, E.; Dahaoui, S.; Fertey, P.; Lebègue, S. b.; Ángyán, J. n. G.; Fourmigué, M.; Espinosa, E., *Cryst. Growth Des.* **2013,** *13* (8), 3283.
32. Bauzá, A.; Quiñonero, D.; Deyà, P. M.; Frontera, A., *CrystEngComm* **2013,** *15* (16), 3137.
33. Adhikari, U.; Scheiner, S., *J. Phys. Chem. A* **2012,** *116* (13), 3487.
34. Scheiner, S., *Int. J. Quantum Chem.* **2013,** *113* (11), 1609.
35. Esrafili, M. D.; Vakili, M., *Mol. Phys.* **2014,** *112* (20), 2746.
36. Azofra, L. M.; Alkorta, I.; Scheiner, S., *J. Phys. Chem. A* **2015,** *119* (3), 535.
37. Esrafili, M. D.; Mohammadian-Sabet, F., *Chem. Phys. Lett.* **2015,** *628*, 71.
38. Adhikari, U.; Scheiner, S., *Chem. Phys. Lett.* **2012,** *532*, 31.
39. Azofra, L. M.; Alkorta, I.; Scheiner, S., *Phys. Chem. Chem. Phys.* **2014,** *16* (35), 18974.
40. Bleiholder, C.; Werz, D. B.; Köppel, H.; Gleiter, R., *J. Am. Chem. Soc.* **2006,** *128* (8), 2666.
41. Bleiholder, C.; Gleiter, R.; Werz, D. B.; Köppel, H., *Inorg. Chem.* **2007,** *46* (6), 2249.
42. Esrafili, M. D.; Mohammadian-Sabet, F., *Struct. Chem.* **2014,** *26* (1), 199.
43. Guo, X.; Liu, Y.-W.; Li, Q.-Z.; Li, W.-Z.; Cheng, J.-B., *Chem. Phys. Lett.* **2015,** *620*, 7.
44. Esrafili, M. D.; Mohammadian-Sabet, F.; Baneshi, M. M., *Can. J. Chem.* **2015,** *93* (11), 1169.
45. Wieczorek, R.; Dannenberg, J., *J. Am. Chem. Soc.* **2003,** *125* (27), 8124.
46. Zhao, Q., *J. Mol. Model.* **2014,** *20* (10), 1.
47. Esrafili, M. D.; Saeidi, N.; Solimannejad, M., *J. Mol. Model.* **2015,** *21* (11), 1.
48. Schmidt, M. W.; Baldridge, K. K.; Boatz, J. A.; Elbert, S. T.; Gordon, M. S.; Jensen, J. H.; Koseki, S.; Matsunaga, N.; Nguyen, K. A.; Su, S.; Windus, T. L.; Dupuis, M.; Montgomery, J. A., *J. Comput. Chem.* **1993,** *14* (11), 1347.
49. Boys, S. F.; Bernardi, F., *Mol. Phys.* **1970,** *19* (4), 553.
50. Bulat, F.; Toro-Labbé, A.; Brinck, T.; Murray, J.; Politzer, P., *J. Mol. Model.* **2010,** *16* (11), 1679.
51. Reed, A. E.; Curtiss, L. A.; Weinhold, F., *Chem. Rev.* **1988,** *88* (6), 899.
52. Glendening, E.; Badenhoop, J.; Reed, A.; Carpenter, J.; Bohmann, J.; Morales, C.; Weinhold, F., *Theoretical Chemistry Institute, University of Wisconsin, Madison* **2001**.
53. Bader, R. F. W. *Atoms in Molecules: A Quantum Theory*. Oxford University Press: New York, 1990.
54. Biegler-Konig, F.; Schonbohm, J.; Bayles, D. Vol. 22 John Wiley & Sons Inc., 605 Third Ave., New York, NY 10158-0012 USA 2001; pp 545.
55. Wolinski, K.; Hinton, J. F.; Pulay, P., *J. Am. Chem. Soc.* **1990,** *112* (23), 8251.
56. Jing, B.; Li, Q.; Gong, B.; Li, R.; Liu, Z.; Li, W.; Cheng, J.; Sun, J., *Int. J. Quantum Chem.* **2012,** *112* (5), 1491.
57. Li, Q.; Guo, X.; Yang, X.; Li, W.; Cheng, J.; Li, H.-B., *Phys. Chem. Chem. Phys.* **2014,** *16* (23), 11617.
58. Li, Q.; Zhuo, H.; Yang, X.; Cheng, J.; Li, W.; Loffredo, R. E., *ChemPhysChem* **2014,** *15* (3), 500.
59. Li, Q.; Wang, Y.; Li, W.; Cheng, J.; Gong, B.; Sun, J., *Phys. Chem. Chem. Phys.* **2009,** *11* (14), 2402.

60. Li, Q.-Z.; Li, R.; Liu, X.-F.; Li, W.-Z.; Cheng, J.-B., *J. Phys. Chem. A* **2012,** *116* (10), 2547.
61. Esrafili, M. D.; Solimannejad, M., *J. Mol. Model.* **2013,** *19* (9), 3767.
62. Li, Q.; Li, R.; Liu, Z.; Li, W.; Cheng, J., *J. Comput. Chem.* **2011,** *32* (15), 3296.
63. Scheiner, S., *Acc. Chem. Res.* **2012,** *46* (2), 280.
64. Rozas, I.; Alkorta, I.; Elguero, J., *J. Am. Chem. Soc.* **2000,** *122* (45), 11154.
65. Alkorta, I.; Elguero, J.; Del Bene, J. E., *J. Phys. Chem. A* **2013,** *117* (40), 10497.
66. Alkorta, I.; Elguero, J.; Del Bene, J. E., *J. Phys. Chem. A* **2013,** *117* (23), 4981.
67. Koch, U.; Popelier, P., *J. Phys. Chem.* **1995,** *99* (24), 9747.

Table 1. . The most positive ($V_{S,max}$, kcal/mol) and most negative ($V_{S,min}$, kcal/mol) electrostatic potentials calculated on the surface of molecular electron density at the 0.001 electrons Bohr $^{-3}$ of the monomers

monomer	$V_{S,max}$	$V_{S,min}$
FHS	48.2	-
ClHS	35.7	-
BrHS	31.4	-
FHSe	55.5	-
ClHSe	42.6	-
BrHSe	37.6	-
NCH	58.7	-33.5
LiH	-	-53.0
NaH	-	-56.9
HBeH	-	-13.6
HMgH	-	-24.8

Table 2. Binding distances (R, Å) of chalcogen bond and DHB bond in the dyads and triads (T), and their changes (ΔR, Å)

Complex (A···B···C)	R_{AB}	R_{AB}(T)	ΔR_{AB}	R_{BC}	R_{BC}(T)	ΔR_{BC}
FHS···NCH···HLi	2.641	2.544	-0.097	1.773	1.699	-0.074
FHS ···NCH···HNa	2.641	2.529	-0.112	1.760	1.675	-0.085
FHS ···NCH···HBeH	2.641	2.620	-0.021	2.030	1.985	-0.045
FHS ···NCH···HMgH	2.641	2.600	-0.041	1.924	1.871	-0.053
ClHS···NCH···HLi	2.849	2.758	-0.091	1.773	1.716	-0.057
ClHS ···NCH···HNa	2.849	2.742	-0.107	1.760	1.694	-0.066
ClHS ···NCH···HBeH	2.849	2.829	-0.020	2.030	1.996	-0.034
ClHS ···NCH···HMgH	2.849	2.810	-0.039	1.924	1.883	-0.041
BrHS···NCH···HLi	2.888	2.800	-0.088	1.773	1.719	-0.054
BrHS ···NCH···HNa	2.888	2.784	-0.104	1.760	1.699	-0.061
BrHS ···NCH···HBeH	2.888	2.869	-0.019	2.030	1.997	-0.033
BrHS ···NCH···HMgH	2.888	2.852	-0.036	1.924	1.886	-0.038
FHSe···NCH···HLi	2.566	2.471	-0.095	1.773	1.667	-0.106
FHSe ···NCH···HNa	2.566	2.456	-0.110	1.760	1.637	-0.123
FHSe ···NCH···HBeH	2.566	2.544	-0.022	2.030	1.962	-0.068
FHSe ···NCH···HMgH	2.566	2.525	-0.041	1.924	1.846	-0.078
ClHSe···NCH···HLi	2.748	2.636	-0.112	1.773	1.687	-0.086
ClHSe ···NCH···HNa	2.748	2.612	-0.136	1.760	1.658	-0.102
ClHSe ···NCH···HBeH	2.748	2.723	-0.025	2.030	1.977	-0.053
ClHSe ···NCH···HMgH	2.748	2.699	-0.049	1.924	1.862	-0.062
BrHSe···NCH···HLi	2.796	2.681	-0.115	1.773	1.692	-0.081
BrHSe···NCH···HNa	2.796	2.661	-0.135	1.760	1.665	-0.095
BrHSe ···NCH···HBeH	2.796	2.770	-0.026	2.030	1.980	-0.050
BrHSe ···NCH···HMgH	2.796	2.747	-0.049	1.924	1.866	-0.058

Table 3. Interaction energies (E_{int}, kcal/mol) of chalcogen bond and DHB in the binary and ternary (T) complexes and cooperative energies (E_{coop}, kcal/mol) [a]

Complex (A···B···C)	E_{int}(AB)	E_{int}(BC)	E_{int}(AB, T)	E_{int}(BC, T)	E_{int}(AC, T)	E_{int} (ABC)	E_{coop}
FHS···NCH···HLi	-5.18	-8.76	-6.68	-10.36	-0.62	-16.09	-1.53
FHS ···NCH···HNa	-5.18	-9.68	-6.95	-11.63	-0.71	-17.42	-1.85
FHS ···NCH···HBeH	-5.18	-2.01	-5.50	-2.31	-0.09	-7.58	-0.30
FHS ···NCH···HMgH	-5.18	-3.88	-5.81	-4.50	-0.18	-9.86	-0.62
ClHS···NCH···HLi	-3.83	-8.76	-4.95	-9.99	-0.46	-14.21	-1.16
ClHS ···NCH···HNa	-3.83	-9.68	-5.15	-11.18	-0.53	-15.44	-1.40
ClHS ···NCH···HBeH	-3.83	-2.01	-4.07	-2.24	-0.07	-6.14	-0.23
ClHS ···NCH···HMgH	-3.83	-3.88	-4.30	-4.35	-0.14	-8.32	-0.47
BrHS···NCH···HLi	-3.45	-8.76	-4.46	-9.92	-0.39	-13.65	-1.05
BrHS ···NCH···HNa	-3.45	-9.68	-4.64	-11.09	-0.45	-14.85	-1.27
BrHS ···NCH···HBeH	-3.45	-2.01	-3.66	-2.22	-0.06	-5.72	-0.20
BrHS ···NCH···HMgH	-3.45	-3.88	-3.87	-4.32	-0.12	-7.87	-0.42
FHSe···NCH···HLi	-6.69	-8.76	-9.38	-11.62	-0.33	-18.49	-2.71
FHSe ···NCH···HNa	-6.69	-9.68	-9.88	-13.16	-0.36	-20.02	-3.29
FHSe ···NCH···HBeH	-6.69	-2.01	-7.22	-2.51	-0.06	-9.25	-1.26
FHSe ···NCH···HMgH	-6.69	-3.88	-7.73	-4.92	-0.11	-11.69	-2.01
ClHSe···NCH···HLi	-4.93	-8.76	-6.98	-11.05	-0.31	-16.09	-2.09
ClHSe ···NCH···HNa	-4.93	-9.68	-7.02	-12.13	-0.33	-17.51	-2.57
ClHSe ···NCH···HBeH	-4.93	-2.01	-5.32	-2.39	-0.05	-7.36	-0.37
ClHSe ···NCH···HMgH	-4.93	-3.88	-5.71	-4.69	-0.10	-9.68	-0.77
BrHSe···NCH···HLi	-4.37	-8.76	-5.93	-10.61	-0.26	-15.26	-1.87
BrHSe···NCH···HNa	-4.37	-9.68	-6.53	-12.27	-0.32	-16.62	-2.25
BrHSe ···NCH···HBeH	-4.37	-2.01	-4.71	-2.36	-0.05	-6.75	-0.32
BrHSe ···NCH···HMgH	-4.37	-3.88	-5.05	-4.61	-0.10	-9.02	-0.67

[a] In each ternary complex, $E_{int,AC(T)}$ refers to the interaction energy of AC pair in the optimized geometry.

Table 4. The electron density (ρ_{BCP}, au) and its Laplacian ($\nabla^2\rho_{BCP}$, au) at the Y···N and H···H BCPs of the binary and ternary (T) complexes

Complex (A···B···C)	ρ_{BCP} (AB)	ρ_{BCP} (AB,T)	ρ_{BCP} (BC)	ρ_{BCP} (BC,T)	$\nabla^2\rho_{BCP}$ (AB)	$\nabla^2\rho_{BCP}$ (AB,T)	$\nabla^2\rho_{BCP}$ (BC)	$\nabla^2\rho_{BCP}$ (BC,T)
FHS···NCH···HLi	0.021	0.026	0.020	0.023	0.087	0.101	0.041	0.043
FHS ···NCH···HNa	0.021	0.027	0.021	0.025	0.087	0.103	0.039	0.041
FHS ···NCH···HBeH	0.021	0.022	0.009	0.010	0.087	0.090	0.028	0.030
FHS ···NCH···HMgH	0.021	0.023	0.013	0.015	0.087	0.093	0.033	0.036
ClHS···NCH···HLi	0.014	0.017	0.020	0.022	0.061	0.073	0.041	0.043
ClHS ···NCH···HNa	0.014	0.018	0.021	0.024	0.061	0.075	0.039	0.041
ClHS ···NCH···HBeH	0.014	0.014	0.009	0.010	0.061	0.064	0.028	0.030
ClHS ···NCH···HMgH	0.014	0.015	0.013	0.014	0.061	0.066	0.033	0.035
BrHS···NCH···HLi	0.013	0.016	0.020	0.022	0.057	0.068	0.041	0.043
BrHS ···NCH···HNa	0.013	0.016	0.021	0.024	0.057	0.070	0.039	0.041
BrHS ···NCH···HBeH	0.013	0.014	0.009	0.010	0.057	0.060	0.028	0.030
BrHS ···NCH···HMgH	0.013	0.014	0.013	0.014	0.057	0.062	0.033	0.035
FHSe···NCH···HLi	0.027	0.034	0.020	0.025	0.101	0.114	0.041	0.044
FHSe ···NCH···HNa	0.027	0.035	0.021	0.027	0.101	0.116	0.039	0.042
FHSe ···NCH···HBeH	0.027	0.029	0.009	0.011	0.101	0.104	0.028	0.032
FHSe ···NCH···HMgH	0.027	0.030	0.013	0.016	0.101	0.106	0.033	0.037
ClHSe···NCH···HLi	0.019	0.025	0.020	0.024	0.076	0.090	0.041	0.044
ClHSe ···NCH···HNa	0.019	0.018	0.021	0.024	0.076	0.075	0.039	0.041
ClHSe ···NCH···HBeH	0.019	0.020	0.009	0.011	0.076	0.079	0.028	0.031
ClHSe ··NCH···HMgH	0.019	0.022	0.013	0.015	0.076	0.082	0.033	0.037
BrHSe···NCH···HLi	0.018	0.016	0.020	0.022	0.070	0.068	0.041	0.043
BrHSe···NCH···HNa	0.018	0.024	0.021	0.026	0.070	0.087	0.039	0.041
BrHSe ···NCH···HBeH	0.018	0.019	0.009	0.010	0.070	0.073	0.028	0.031
BrHSe ···NCH···HMgH	0.018	0.020	0.013	0.014	0.070	0.079	0.033	0.030

Table 5. NBO charge-transfer energies ($E^{(2)}$, kcal/mol) and the net transferred charge (Q_{CT}, e) of the binary and ternary (T) complexes

Complex (A···B···C)	$E^{(2)}_{AB}$	$E^{(2)}_{AB}$(T)	$E^{(2)}_{BC}$	$E^{(2)}_{BC}$(T)	$Q_{CT,AB}$	$Q_{CT,AB}$(T)	$Q_{CT,BC}$	$Q_{CT,BC}$(T)
FHS···NCH···HLi	8.61	12.79	14.96	19.77	0.013	0.024	0.030	0.040
FHS ···NCH···HNa	8.61	13.60	17.93	24.44	0.013	0.026	0.041	0.056
FHS ···NCH···HBeH	8.61	9.35	2.15	2.68	0.013	0.015	0.003	0.004
FHS ···NCH···HMgH	8.61	10.13	5.75	7.22	0.013	0.017	0.011	0.014
ClHS···NCH···HLi	4.12	6.22	14.96	18.48	0.007	0.014	0.030	0.037
ClHS ···NCH···HNa	4.12	6.66	17.93	22.67	0.007	0.015	0.041	0.052
ClHS ···NCH···HBeH	4.12	4.50	2.15	2.53	0.007	0.008	0.003	0.004
ClHS ···NCH···HMgH	4.12	4.87	5.75	6.82	0.007	0.009	0.011	0.013
BrHS···NCH···HLi	3.58	5.46	14.96	18.22	0.006	0.012	0.030	0.037
BrHS ···NCH···HNa	3.58	5.84	17.93	22.31	0.006	0.013	0.041	0.052
BrHS ···NCH···HBeH	3.58	3.91	2.15	2.51	0.006	0.007	0.003	0.004
BrHS ···NCH···HMgH	3.58	4.22	5.75	6.74	0.006	0.008	0.011	0.013
FHSe···NCH···HLi	16.47	23.77	14.96	22.36	0.023	0.004	0.030	0.045
FHSe ···NCH···HNa	16.47	25.18	17.93	28.04	0.023	0.045	0.041	0.064
FHSe ···NCH···HBeH	16.47	17.89	2.15	3.01	0.023	0.027	0.003	0.005
FHSe ···NCH···HMgH	16.47	19.27	5.75	8.06	0.023	0.030	0.011	0.016
ClHSe···NCH···HLi	9.71	15.19	14.96	20.62	0.016	0.029	0.030	0.042
ClHSe ···NCH···HNa	9.71	16.53	17.93	25.88	0.016	0.032	0.041	0.059
ClHSe ···NCH···HBeH	9.71	10.71	2.15	2.77	0.016	0.018	0.003	0.005
ClHSe ···NCH···HMgH	9.71	11.72	5.75	7.47	0.016	0.020	0.011	0.015
BrHSe···NCH···HLi	8.40	13.39	14.96	20.17	0.014	0.026	0.030	0.040
BrHSe···NCH···HNa	8.40	14.49	17.93	25.17	0.014	0.029	0.041	0.058
BrHSe ···NCH···HBeH	8.40	9.31	2.15	2.72	0.014	0.016	0.003	0.004
BrHSe ···NCH···HMgH	8.40	10.41	5.75	6.64	0.014	0.018	0.011	0.012

Table 6. NMR chemical shielding (σ , ppm) and spin-spin coupling constants (J, Hz) of the binary complexes and their changes in the ternary systems

Complex	$\sigma(^{15}N)$	$\sigma(^{1}H)$	J(Y-N)	J(H-H)	$\Delta\sigma(^{15}N)$	$\Delta\sigma(^{1}H)$	ΔJ(Y-N)	ΔJ(H-H)
FHS···NCH···HLi	68.0	24.5	13.7	2.0	-21.7	-1.0	1.3	1.5
FHS ···NCH···HNa	68.0	23.8	13.7	5.8	-25.1	-1.4	1.8	1.7
FHS ···NCH···HBeH	68.0	28.5	13.7	0.3	-4.8	-0.2	0.3	0.5
FHS ···NCH···HMgH	68.0	27.2	13.7	2.4	-9.3	-0.4	0.8	0.8
ClHS···NCH···HLi	73.1	24.5	9.6	2.0	-20.5	-0.8	1.0	2.3
ClHS ···NCH···HNa	73.1	23.8	9.6	5.8	-23.6	-1.1	1.3	2.5
ClHS ···NCH···HBeH	73.1	28.5	9.6	0.3	-4.6	-0.2	0.2	0.5
ClHS ···NCH···HMgH	73.1	27.2	9.6	2.4	-8.9	-0.4	0.7	0.9
BrHS···NCH···HLi	74.3	24.5	8.7	2.0	-20.3	-0.8	0.9	1.9
BrHS ···NCH···HNa	74.3	23.8	8.7	5.8	-23.4	-1.0	1.3	2.3
BrHS ···NCH···HBeH	74.3	28.5	8.7	0.3	-4.5	-0.2	0.2	0.3
BrHS ···NCH···HMgH	74.3	27.2	8.7	2.4	-8.8	-0.3	0.6	0.6
FHSe···NCH···HLi	61.4	24.5	18.2	2.0	-24.1	-1.6	1.9	4.6
FHSe ···NCH···HNa	61.4	23.8	18.2	5.8	-28.0	-2.1	3.0	5.1
FHSe ···NCH···HBeH	61.4	28.5	18.2	0.3	-5.4	-0.4	0.4	1.1
FHSe ···NCH···HMgH	61.4	27.2	18.2	2.4	-10.4	-0.7	1.2	1.9
ClHSe···NCH···HLi	67.3	24.5	13.1	2.0	-23.0	-1.3	1.5	2.1
ClHSe ···NCH···HNa	67.3	23.8	13.1	5.8	-26.8	-1.8	2.3	2.9
ClHSe ···NCH···HBeH	67.3	28.5	13.1	0.3	-5.2	-0.3	0.3	0.7
ClHSe ···NCH···HMgH	67.3	27.2	13.1	2.4	-9.9	-0.6	1.0	1.2
BrHSe···NCH···HLi	69.0	24.5	10.8	2.0	-22.6	-1.2	1.4	2.4
BrHSe···NCH···HNa	69.0	23.8	10.8	5.8	-26.2	-1.6	2.2	2.8
BrHSe ···NCH···HBeH	69.0	28.5	10.8	0.3	-5.1	-0.3	0.3	0.4
BrHSe ···NCH···HMgH	69.0	29.2	10.8	2.4	-14.5	-0.5	0.6	1.0

Figure 1. Calculated MEPs of the isolated SHF, NCH, LiH and HBeH monomers. The color code ranges from blue (more negative) to red (more positive). The locations of the surface maxima and minima are indicated with black and blue circles, respectively.

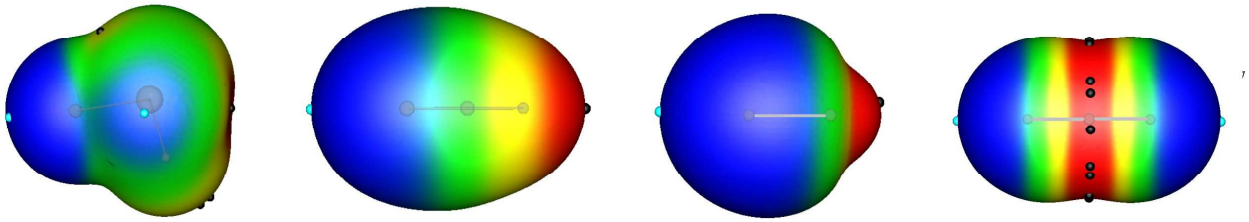

SHF NCH LiH HBeH

Figure 2. Exponential relationship between the binding distances and electron densities at the BCPs of the ternary systems